Study of $B \to D^{(*)}\ell\bar{\nu}$ semileptonic decays by using lattice QCD

Jaehoon Leem
Korea Institute for Advanced Study

The 1st AEI Workshop for BSM and
the 9th KIAS Workshop on
Particle Physics and Cosmology
Nov. 4-8, 2019

SWME-LNAL collaboration

Los Alamos National Laboratory

- Sungwoo Park
- Rajan Gupta
- Tanmoy Bhattacharya

Brookhaven National Laboratory

- Yong-Chull Jang

Seoul National University

- Weonjong Lee
- Jon A. Bailey
- Jaedon Choi
- Sunkyu Lee
- Seung-Yeob Jwa

Korea Institute for Advanced Study

- Jaehoon Leem (Speaker)

Motivation

- $B \to D^{(*)}\ell\bar{\nu}$ decays : determine $|V_{cb}|$.
- $|V_{cb}|$: long-standing tension between inclusive and exclusive determinations.
- $R(D)$ and $R(D^*)$: 2σ-3σ tension with the SM.
- Expect increasing precision in experiment : Belle II, LHCb

What is role of the Lattice QCD in understanding these issues?

Exclusive determination of $|V_{cb}|$: $\bar{B} \to D^* \ell \bar{\nu}$ I

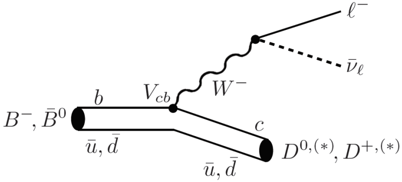

1703.01766

$$\frac{d\Gamma}{dw}(\bar{B} \to D\ell\bar{\nu}) = \frac{G_F^2 m_D^3}{48\pi^3}(m_B + m_D)^2 (w^2 - 1)^{3/2} \eta_{\mathrm{EW}}^2 |V_{cb}|^2 \mathcal{G}(w)^2$$

$$\frac{d\Gamma}{dw}(\bar{B} \to D^*\ell\bar{\nu}) = \frac{G_F^2 m_{D^*}^3}{48\pi^3}(m_B - m_{D^*})^2 (w^2 - 1)^{1/2} \eta_{\mathrm{EW}}^2 |V_{cb}|^2 \chi(w) \mathcal{F}(w)^2$$

where the recoil parameter w is

$$w \equiv v_B \cdot v_{D^{(*)}} = \frac{m_B^2 + m_{D^{(*)}}^2 - q^2}{2 m_B m_{D^{(*)}}} \left(= \frac{E_{D^{(*)}}}{m_{D^{(*)}}}, \quad \text{when } \bar{B} \text{ is at rest} \right)$$

Exclusive determination of $|V_{cb}|$: $\bar{B} \to D^* \ell \bar{\nu}$ II

- Lattice QCD : calculate hadronic matrix elements & determine $\mathcal{F}(w)$, $\mathcal{G}(w)$.

$$\frac{\langle D|V^\mu|\bar{B}\rangle}{\sqrt{m_B m_D}} = (v_B + v_D)^\mu h_+(w) + (v_B - v_D)^\mu h_-(w),$$

$$\frac{\langle D^*|V^\mu|\bar{B}\rangle}{\sqrt{m_B m_{D^*}}} = h_V(w)\epsilon^{\mu\nu\alpha\beta}\epsilon^{*\nu} v^\alpha_{D^*} v^\beta_B,$$

$$\frac{\langle D^*|A^\mu|\bar{B}\rangle}{\sqrt{m_B m_{D^*}}} = -i h_{A_1}(w)(w+1)\epsilon^{*\mu} + i h_{A_2}(w)(\epsilon^* \cdot v_B) v^\mu_B + i h_{A_3}(w)(\epsilon^* \cdot v_B) v^\mu_{D^*}$$

At zero recoil ($v_B = v_{D^{(*)}}$, $w = 1$), $\mathcal{F}(1) = h_{A_1}(1)$.

- Determination of CKM matrix elements with lattice QCD

Decay rate (exp.) = known factors $\times |V_{CKM}|^2 \times$ Hadronic matrix elements

Exclusive determination of $|V_{cb}|$: $\bar{B} \to D^* \ell \bar{\nu}$ III

- LQCD calculations are more precise near zero recoil ($w \simeq 1$), whereas experimental data for decay rate is suppressed by factor $(w^2 - 1)^{1/2}$ or $(w^2 - 1)^{3/2}$.
- Connect LQCD & experiment : extrapolation to the zero recoil is required.

$$|V_{cb}|\mathcal{F}(w \simeq 1) \to |V_{cb}|\mathcal{F}(1),$$

- Parametrization dependence? : CLN vs. BGL

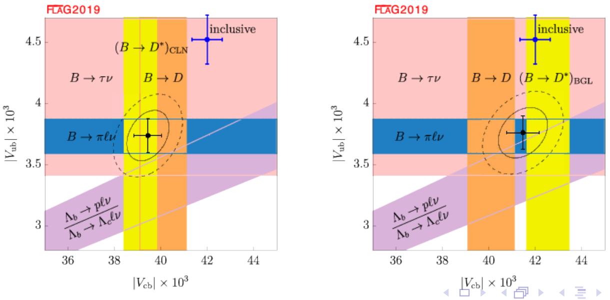

$\bar{B} \to D^{(*)}\ell\bar{\nu}$ Form Factor Parametrization: CLN vs. BGL I

- CLN (Caprini, Lellouch, and Neubert) [NPB.530, 153] : HQET frameworks

$$\left[1+\frac{4w}{w+1}\frac{1-2wr+r^2}{(1-r)^2}\right]\mathcal{F}^2(w) = h_{A_1}^2(w)\left\{2\frac{1-2wr+r^2}{(1-r)^2}\left[1+\frac{w-1}{w+1}R_1^2(w)\right] + \left[1+\frac{w-1}{1-r}\Big(1-R_2(w)\Big)\right]^2\right\}, \qquad (r = m_{D^*}/m_B).$$

$$R_1(w) = R_1(1) - 0.12(w-1) + 0.05(w-1)^2$$

$$R_2(w) = R_2(1) + 0.11(w-1) - 0.06(w-1)^2$$

$$h_{A_1}(w) = h_{A_1}(1)\left[1 - 8\rho^2 z + (53\rho^2 - 15)z^2 - (231\rho^2 - 91)z^3\right], \quad \left(z = \frac{\sqrt{w+1}-\sqrt{2}}{\sqrt{w+1}+\sqrt{2}}\right)$$

- BGL (Boyd, Grinstein, and Lebed) [PRD.56,6895] : unitarity constraints

$$f_i(z) = \frac{1}{\phi_i(z)P_i(z)}\sum_{k=0}^{n_i} a_k^i z^k, \quad (\text{with } f_i(z) = H_0(z), H_\pm(z) : \text{Helicity amplitudes})$$

CLN vs. BGL

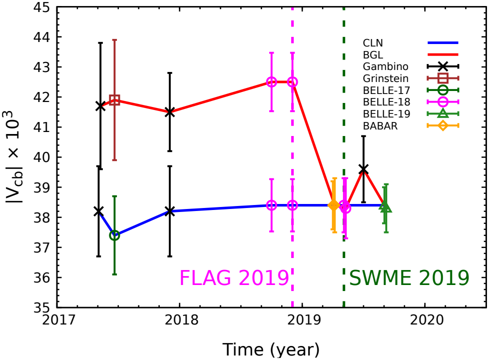

(plot by W. Lee)

- Belle 2018 : difference between CLN/BGL,

$$|V_{cb}| = 42.5 \pm 0.6 \times 10^{-3}(\mathrm{BGL} + \mathrm{LQCD})$$
$$|V_{cb}| = 38.4 \pm 0.6 \times 10^{-3}(\mathrm{CLN} + \mathrm{LQCD})$$

CLN vs. BGL

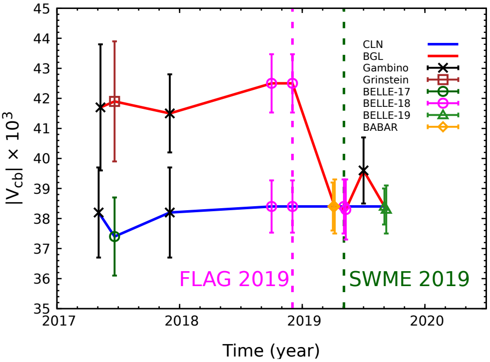

(plot by W. Lee)

- Belle 2019 : the BGL result converges to the CLN result

$$|V_{cb}| = 38.3 \pm 0.7 \times 10^{-3}(\text{BGL} + \text{LQCD})$$
$$|V_{cb}| = 38.4 \pm 0.6 \times 10^{-3}(\text{CLN} + \text{LQCD})$$

CLN vs. BGL

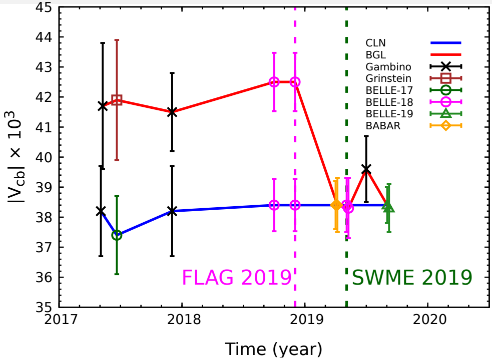

(plot by W. Lee)

- Belle 2019 : the BGL result converges to the CLN result

$$|V_{cb}| = 38.3 \pm 0.7 \times 10^{-3}(\text{BGL} + \text{LQCD})$$
$$|V_{cb}| = 38.4 \pm 0.6 \times 10^{-3}(\text{CLN} + \text{LQCD})$$

- BABAR 2019 : analysis with BGL/CLN, consistent with Belle 2019
- Gambino (1905.08209): BGL with more fit parameters $\text{BGL}_{102} \rightarrow \text{BGL}_{222}$

$R_1(w)$ and $R_2(w)$: JLQCD results

$R_1(w) \equiv \frac{h_V(w)}{h_{A_1}(w)}$, $R_2(w) \equiv \frac{h_{A_3}(w)+rh_{A_2}(w)}{h_{A_1}(w)}$, with $(r = M_{D^*}/M_B)$

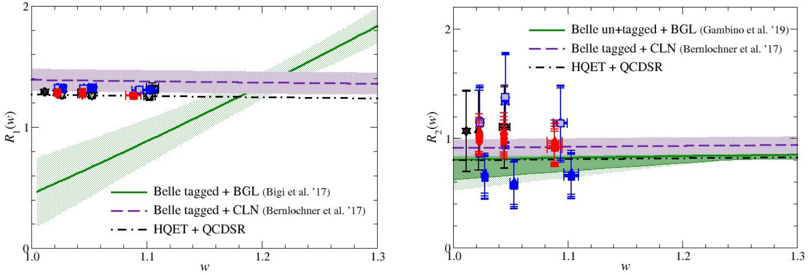

plots from T. Kaneko's talk (Lattice 2019)

$R_1(w)$ and $R_2(w)$: JLQCD results

$R_1(w) \equiv \frac{h_V(w)}{h_{A_1}(w)}$, $R_2(w) \equiv \frac{h_{A_3}(w)+rh_{A_2}(w)}{h_{A_1}(w)}$, with $(r = M_{D^*}/M_B)$

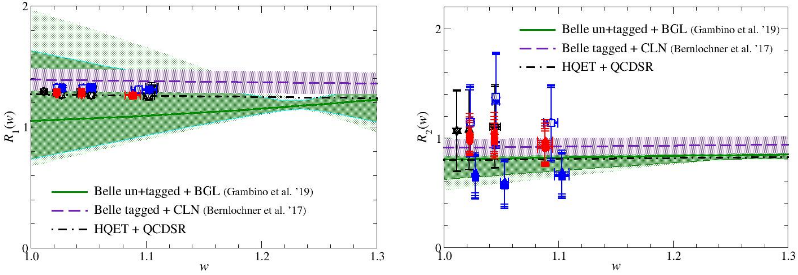

plots from T. Kaneko's talk (Lattice 2019)

$R_1(w)$ and $R_2(w)$: JLQCD results

$$R_1(w) \equiv \frac{h_V(w)}{h_{A_1}(w)},\ R_2(w) \equiv \frac{h_{A_3}(w)+rh_{A_2}(w)}{h_{A_1}(w)},\ \text{with } (r = M_{D^*}/M_B)$$

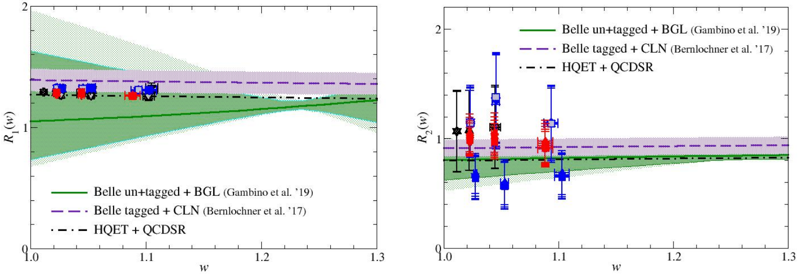

plots from T. Kaneko's talk (Lattice 2019)

- JLQCD's results for $R_1(w)$ favor the CLN result.
- CLN/BGL : $R_1(w)$ and $R_2(w)$ are determined by fitting.
- LQCD results of $R_1(w)$ and $R_2(w)$ can be input parameters of the parametrization and enhance the extrapolation.

$|V_{cb}|$ puzzle : unresolved

Table: $|V_{cb}|$ in units of 1.0×10^{-3}.

(a) Exclusive $|V_{cb}|$

channel	value	Ref.
CLN	38.4(8)	BABAR 2019
BGL	38.4(9)	BABAR 2019
CLN	38.4(6)	Belle 2019
BGL	38.3(8)	Belle 2019
CLN	39.13(59)	HFLAV 2017
CLN	39.25(56)	HFLAV 2019 [Web][1]

(b) Inclusive $|V_{cb}|$

channel	value	Ref.
kinetic scheme	42.19(78)	HFLAV 2017
1S scheme	41.98(45)	HFLAV 2017

(BABAR 2019 : 1903.10002), (Belle 2019 : PRD 100, 052007 (2019)), (HFLAV 2017 : EPJ.C77, 895 (2017))

- $3\sigma \sim 4\sigma$ difference in $|V_{cb}|$ between the exclusive and inclusive decay channels : the $|V_{cb}|$ puzzle is unresolved yet.

[1] Preliminary !!

Current status of $|V_{cb}|$

- Combined fit of exclusive $|V_{ub}|$ and $|V_{cb}|$ (preliminary)

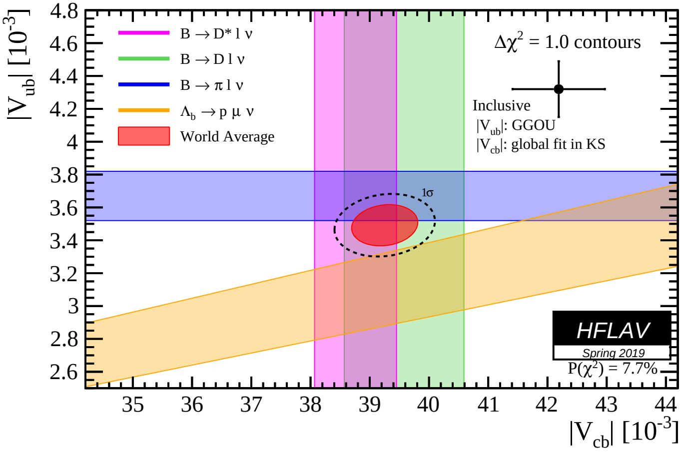

$R(D)$ and $R(D^*)$

- R-ratios for $B \to D^{(*)}$ semileptonic decay

$$R(D) \equiv \frac{\mathcal{B}(B \to D\tau\nu_\tau)}{\mathcal{B}(B \to D\ell\nu_\ell)}, \qquad R(D^*) \equiv \frac{\mathcal{B}(B \to D^*\tau\nu_\tau)}{\mathcal{B}(B \to D^*\ell\nu_\ell)}$$

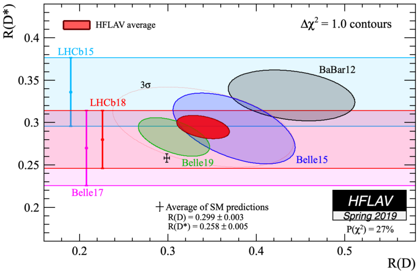

- Results of HFLAV 2019 (Preliminary)

channel	SM	Experiment	Difference
$R(D)$	0.299(3)	0.340(27)(13)	1.4σ
$R(D^*)$	0.258(5)	0.295(11)(8)	2.5σ

$R(D)$ and $R(D^*)$ by LQCD

- Calculate semi-leptonic form factors at zero recoil and non-zero recoil points. By fitting the data, we obtain form factors ($\mathcal{F}(w)$ and $\mathcal{G}(w)$) for the full range of w using parametetrization like CLN, BGL.

- The recoil parameter w has bound as

$$1 \le w = v_B \cdot v_D = \frac{m_B^2 + m_D^2 - q^2}{2 m_B m_D} \le w_{\max}^{\ell(\tau)} = \frac{m_B^2 + m_D^2 - m_{\ell(\tau)}^2}{2 m_B m_D}$$

$$R(D^*) = \frac{\mathcal{B}(B \to D^* \tau \nu_\tau)}{\mathcal{B}(B \to D^* \ell \nu_\ell)} = \frac{\displaystyle\int_1^{w_{\max}^{\tau}} dw \left[\frac{d\Gamma}{dw}(w, m_\tau)\right]}{\displaystyle\int_1^{w_{\max}^{\ell}} dw \left[\frac{d\Gamma}{dw}(w, m_\ell)\right]}, \quad \text{where} \quad \ell = \{e,\ \mu\},$$

$$w_{\max}^{\tau} = 1.355, \quad w_{\max}^{\ell} = 1.503$$

- Integrate using ($|V_{cb}|^2$ is cancelled out)

$$\frac{d\Gamma}{dw} \propto \text{known factors} \times \mathcal{F}^2(w)$$

Study of $\bar{B} \to D^{(*)}\ell\bar{\nu}$ on the lattice

1. Exclusive $\bar{B} \to D^*\ell\bar{\nu}$ at zero recoil [Fermilab-MILC (2014), HPQCD (2018)]
   - Most precise in experimental and lattice errors.
   - The decay rate depends on a single form factor h_{A_1}. Form factor calculation using the 3-point function $\langle D^*|A^\mu|B\rangle$ on the lattice.
2. Exclusive $\bar{B} \to D\ell\bar{\nu}$ at non-zero recoil [Fermilab-MILC (2015), HPQCD (2015)]
   - Near the zero recoil, the experimental precision is poor due to to the phase space suppression.
   - Form factor calculation using the 3-point function $\langle D|V^\mu|B\rangle$ on the lattice.

Decay mode	Method	$\lvert V_{cb}\rvert \times 10^3$ [HFLAV (2017)]
$\bar{B} \to D^*\ell\bar{\nu}$	Lattice	39.05(47)(58)
$\bar{B} \to D\ell\bar{\nu}$	Lattice	39.18(94)(36)
$B \to X_c\ell\bar{\nu}$	QCD sum rule	42.03(39)

How to control discretization error

- On the lattice, we have **discretization error** by construction.
- For the $\bar{B} \to D^* \ell \bar{\nu}$ study, the heavy quark discretization error for charm quark is dominant.
- **Fermilab action** : Fermilab-MILC (2014) uses the Fermilab action for the b and c quarks.
  The discretization error of $h_{A_1}(1)$: combined error $\mathcal{O}(\alpha_s \lambda^2)$ & $\mathcal{O}(\lambda^3) \sim 1\%$.

  λ : power counting parameter $\quad (\lambda \simeq \Lambda_{\mathrm{QCD}}/2m_Q, \Lambda_{\mathrm{QCD}}\, a)$
- **Oktay-Kronfeld action** : improved version of the Fermilab action. ($\mathcal{O}(\lambda^3)$ improved)

How to control discretization error

- We expect the improvement in charm quark discretization error from the Fermilab/MILC results [PRD89, 114504 (2014)] for the $\bar{B} \to D^{(*)}\ell\bar{\nu}$ semileptonic form factors.

form factor	h_{A_1}
decay channel	$\bar{B} \to D^{*}\ell\bar{\nu}$
statistics	0.4
matching	0.4
χPT	0.5
c discretization	$1.0 \to (0.2)_{\rm OK}$
...	...
total	$1.4 \to (0.8)_{\rm OK}$

- Expect improvement in experiment : Belle II has been running since April, 2019, and the target statistics is 50 times larger than Belle.

Fermilab action

- The Fermilab action [El-Khadra, Kronfeld, and Mackenzie, PRD55, 3933 (1997)]

$$S_{\text{Fermilab}} \equiv S_0 + S_E + S_B,$$

$$S_0 \equiv a^4 \sum_x \bar{\psi}(x) \left[m_0 + \gamma_4 D_{\text{lat},4} - \frac{a}{2}\Delta_4 + \zeta \left(\boldsymbol{\gamma} \cdot \boldsymbol{D}_{\text{lat}} - \frac{r_s a}{2}\Delta^{(3)} \right) \right] \psi(x)$$

$$S_E \equiv -\frac{1}{2} c_E \zeta a^5 \sum_x \bar{\psi}(x) \boldsymbol{\alpha} \cdot \boldsymbol{E}_{\text{lat}} \psi(x), \quad S_B \equiv -\frac{1}{2} c_B \zeta a^5 \sum_x \bar{\psi}(x) i \boldsymbol{\Sigma} \cdot \boldsymbol{B}_{\text{lat}} \psi(x),$$

$\Delta^{(3)}, \Delta_4$: discretized versions of $\boldsymbol{D}^2$, D_4^2.

- Coefficients in the action $(m_0, c_B, \cdots)$ are tuned to reduce the discretization error in $\mathcal{O}(\lambda)$.

Oktay-Kronfeld action

- Oktay-Kronfeld (OK) action : $\mathcal{O}(\lambda) \to \mathcal{O}(\lambda^3)$ improvement. [Oktay and Kronfeld, PRD78, 014504 (2008)]
  $S_{\text{OK}} \equiv S_{\text{Fermilab}} + S_6 + S_7$

$$\begin{aligned} S_6 \equiv\ & c_1 a^6 \sum_x \bar{\psi}(x) \sum_i \gamma_i D_{\text{lat},i} \Delta_i \psi(x) + c_2 a^6 \sum_x \bar{\psi}(x) \{\boldsymbol{\gamma} \cdot \boldsymbol{D}_{\text{lat}}, \Delta^{(3)}\} \psi(x) \\ & + c_3 a^6 \sum_x \bar{\psi}(x) \{\boldsymbol{\gamma} \cdot \boldsymbol{D}_{\text{lat}}, i\boldsymbol{\Sigma} \cdot \boldsymbol{B}_{\text{lat}}\} \psi(x) \\ & + c_{EE} a^6 \sum_x \bar{\psi}(x) \{\gamma_4 D_{\text{lat},4}, \boldsymbol{\alpha} \cdot \boldsymbol{E}_{\text{lat}}\} \psi(x), \end{aligned} \tag{1}$$

$$S_7 \equiv a^7 \sum_x \bar{\psi}(x) \sum_i \Big[c_4 \Delta_i^2 \psi(x) + c_5 \sum_{j \neq i} \{ i\Sigma_i B_{\text{lat},i}, \Delta_j \} \Big] \psi(x). \tag{2}$$

- Coefficients c_i are fixed by matching dispersion relation, interaction with background field, and Compton scattering amplitude of on-shell quark through the tree level.

Current improvement

- Simulation with the Fermilab action : current improvement through $\mathcal{O}(\lambda)$. Improved currents are constructed by improved quark fields [El-Khadra, Kronfeld, and Mackenzie, PRD55, 3933]

$$V_\mu = \bar{\Psi}_c \gamma_\mu \Psi_b, \qquad A_\mu = \bar{\Psi}_c \gamma_\mu \gamma_5 \Psi_b,$$

where

$$\Psi_f = e^{m_{1f}a\,a/2}(1 + d_{1f}\, a\boldsymbol{\gamma} \cdot \boldsymbol{D}_{\text{lat}})\psi_f, \quad f = b, c$$

And determine d_{1f} by matching conditions.

- Simulation with the OK action : current improvement through $\mathcal{O}(\lambda^3)$ is required.

Current improvement

- Tree-level relation between QCD operator and HQET operator is given by Foldy-Wouthouysen-Tani transformation

$$b = \left[1 - \frac{\gamma \cdot \boldsymbol{D}}{2m_b} + \cdots\right] h_b,$$

$$\bar{c}\gamma_\mu b \doteq \bar{h}_c \Gamma h_b - \bar{h}_c \gamma_\mu \frac{\gamma \cdot \boldsymbol{D}}{2m_b} h_b + \bar{h}_c \frac{\gamma \cdot \overleftarrow{\boldsymbol{D}}}{2m_c} \gamma_\mu h_b + \cdots$$

- Taking FWT transformation through $\mathcal{O}(1/m_q^3)$ as ansatz, we introduced improved quark field [Jaehoon Leem, arXiv:1711.01777],

$$\begin{aligned}\Psi(x) =& e^{m_1 a/2}\Big[1 + d_1 a\gamma \cdot \boldsymbol{D}_{\text{lat}} + \frac{1}{2} d_2 a^2 \Delta^{(3)} + \frac{1}{2} i d_B a^2 \boldsymbol{\Sigma} \cdot \boldsymbol{B}_{\text{lat}} + \frac{1}{2} d_E a^2 \boldsymbol{\alpha} \cdot \boldsymbol{E}_{\text{lat}} \\ &+ d_{EE} a^3 \{\gamma_4 D_{4\text{lat}}, \boldsymbol{\alpha} \cdot \boldsymbol{E}_{\text{lat}}\} + d_{r_E} a^3 \{\gamma \cdot \boldsymbol{D}_{\text{lat}}, \boldsymbol{\alpha} \cdot \boldsymbol{E}_{\text{lat}}\} \\ &+ \frac{1}{6} d_3 a^3 \gamma_i D_{\text{lat}i} \Delta_i + \frac{1}{2} d_4 a^3 \{\gamma \cdot \boldsymbol{D}_{\text{lat}}, \Delta^{(3)}\} + d_5 a^3 \{\gamma \cdot \boldsymbol{D}_{\text{lat}}, i\boldsymbol{\Sigma} \cdot \boldsymbol{B}_{\text{lat}}\} \\ &+ d_6 a^3 [\gamma_4 D_{4\text{lat}}, \Delta^{(3)}] + d_7 a^3 [\gamma_4 D_{4\text{lat}}, i\boldsymbol{\Sigma} \cdot \boldsymbol{B}_{\text{lat}}]\Big] \psi(x).\end{aligned}$$

Numerical Simulation

Path integral on lattice

- Calculate Green's functions by performing path integral over discretized Euclidean space-time. For example,

$$\langle O_2(x)O_1(0)\rangle = \frac{1}{Z}\int \prod dU d\bar{q} dq e^{-S_{\mathrm{QCD}}^{\mathrm{lat}}} O_2(x)O_1(0)$$

  The field variable $U_\mu(x)$ is **gauge link**.
- The integral over fermionic Grassmann variables gives fermionic determinant. For example, if $O_2 \equiv \bar{b}\gamma_5 d$ and $O_1 \equiv \bar{d}\gamma_5 b$

$$\begin{aligned}\langle O_2(x)O_1(0)\rangle &= \int \frac{1}{Z}\prod dU d\bar{q} dq e^{-S_g^{\mathrm{lat}}} \bar{b}(x)\gamma_5 d(x)\bar{d}(0)\gamma_5 b(0)\prod_q e^{-\sum_q \bar{q}D_q q} \\ &= -\frac{1}{Z}\int \prod dU e^{-S_g^{\mathrm{lat}}} \prod_q \det[D_q]\mathrm{tr}[\gamma_5 D_d^{-1}(x,0)\gamma_5 D_b^{-1}(0,x)] \\ &\to \sum_{i=1}^{N_{\mathrm{MC}}} w(U_i)(-\mathrm{tr}[\gamma_5 D_d^{-1}(x,0)\gamma_5 D_b^{-1}(0,x)])\end{aligned}$$

  if $\prod_q \det[D_q] \geq 0$, one can use **Monte Carlo simulation** with importance sampling with weight factor $w(U) \propto dU e^{-S_g^{\mathrm{lat}}} \prod_q \det[D_q](U)$.

Lattice QCD

Lattice QCD simulations in three steps.

- Generate gauge configuration : make gauge configurations to follow probability density $P(U) \propto w(U)$.
- Measurements : calculate Euclidean Green's function.
  - Compute quark propagators : inverse of matrix with 4(spin) $\times$3(color) $\times V$(lattice vol) rows and columns. (For $V = 48^3 \times 96$ hypercubic lattice, dimension of matrix is over 100 millions.)
  - Calculate correlation functions by contracting quark fields.
- Extract energy spectrum, hadronic matrix elements, $\cdots$

Sea quark and valence quark

- Fermions in Lagrangian : sea quark $\rightarrow$ fermion determinant
- Fermions in the operator : valence quark $\rightarrow$ propagator.

Numerical Simulation

- Sea quarks : Highly-improved-staggered quark (HISQ) action with $N_f = 2+1+1$ flavors. [MILC collab., PRD87, 054505 (2013)]

ID	a(fm)	Volume	am_l	am_s	am_c	$N_{conf} \times N_{src}$
a12m310	0.12	$24^3 \times 64$	0.0102	0.0509	0.635	1053 $\times 3$
a12m220	0.12	$32^3 \times 64$	0.00507	0.0507	0.628	
a12m130	0.12	$48^3 \times 64$	0.00184	0.0507	0.628	
a09m310	0.09	$32^3 \times 96$	0.0074	0.037	0.440	1001 $\times 3$
a09m220	0.09	$48^3 \times 96$	0.00363	0.0363	0.430	
a09m130	0.09	$64^3 \times 96$	0.0012	0.0363	0.432	

- Valence quark for (u, d, s) : HISQ action
- Valence quark for b and c : Oktay-Kronfeld action
- **Calculate 2-point Green's function** : determine the bare masses of b and c numerically by tuning the energy spectrum of lattice meson.
- **Calculate 3-point Green's function** : determine hadronic matrix elements with the improved flavor-changing current.

Green's function

- 2-point (Euclidean) Green's function : extract meson's energy sepctrum

$$C_B^{2\text{pt}}(\boldsymbol{p}) = \sum_{\boldsymbol{x}} e^{i\boldsymbol{p}\cdot\boldsymbol{x}} \langle O_B(t,\boldsymbol{x}) O_B^\dagger(0)\rangle = \sum_n |\langle 0|O_B^\dagger|B_n\rangle|^2 e^{-E_n(\boldsymbol{p})t}$$
$$= |\langle 0|O_B^\dagger|\bar{B}\rangle|^2 e^{-E_0(\boldsymbol{p})t} + |\langle 0|O_B^\dagger|B_1\rangle|^2 e^{-E_1(\boldsymbol{p})t} + \cdots \quad (3)$$

$O_B^\dagger$ (meson interpolating operator) : creates B-meson as acting on vacuum.

- 3-point (Euclidean) Green's function : extract hadronic matrix elements

$$C_{A_j}^{B\to D^*}(t_s,t_f) = \sum_{\boldsymbol{x},\boldsymbol{y}} \langle O_{D^*}(\boldsymbol{x},t_f) A_j^{cb}(\boldsymbol{y},t_s) O_B^\dagger(\boldsymbol{0},0)\rangle$$
$$= \langle 0|O_{D^*}|D^*\rangle\langle\bar{B}|O_B^\dagger|0\rangle\langle D^*|A_j|\bar{B}\rangle e^{-M_B t_s} e^{-M_{D^*}(t_f-t_s)} + \cdots \quad (4)$$

where A_j^{cb} is flavor-changing axial current.

- Do numerical analysis to extract the ground-state contribution out of excited-state contamination.

$\bar{B} \to D^* \ell \bar{\nu}$ at zero recoil

- $h_{A_1}(1)$ determination by LQCD

$$|h_{A_1}(1)|^2 = \frac{\langle D^*|A^j_{cb}|\bar{B}\rangle\langle\bar{B}|A^j_{bc}|D^*\rangle}{\langle D^*|V^4_{cc}|D^*\rangle\langle\bar{B}|V^4_{bb}|\bar{B}\rangle} \times \rho^2_{A_j}, \quad \text{with} \quad \rho^2_{A_j} = \frac{Z^{cb}_{A_j} Z^{bc}_{A_j}}{Z^{cc}_{V_4} Z^{bb}_{V_4}} \simeq 1$$

- We calculate the following 3-point Green's functions ($w = 1$),

$$\begin{aligned} C^{B\to D^*}_{A_j}(t,\tau) &\equiv \sum_{\boldsymbol{x},\boldsymbol{y}} \langle O_{D^*}(0) A^{cb}_j(\boldsymbol{y},t) O^\dagger_B(\boldsymbol{x},\tau)\rangle, \\ C^{D^*\to B}_{A_j}(t,\tau) &\equiv \sum_{\boldsymbol{x},\boldsymbol{y}} \langle O_B(0) A^{bc}_j(\boldsymbol{y},t) O^\dagger_{D^*}(\boldsymbol{x},\tau)\rangle, \\ C^{B\to B}_{V_4}(t,\tau) &\equiv \sum_{\boldsymbol{x},\boldsymbol{y}} \langle O_B(0) V^{bb}_4(\boldsymbol{y},t) O^\dagger_B(\boldsymbol{x},\tau)\rangle, \\ C^{D^*\to D^*}_{V_4}(t,\tau) &\equiv \sum_{\boldsymbol{x},\boldsymbol{y}} \langle O_{D^*}(0) V^{cc}_4(\boldsymbol{y},t) O^\dagger_{D^*}(\boldsymbol{x},\tau)\rangle, \end{aligned} \tag{5}$$

  where O_B and O_{D^*} are meson interpolating operators.

- The currents are given by the improved quark fields

$$A^{cb}_j \equiv \bar{\Psi}_c \gamma_5 \gamma_j \Psi_b, \qquad V^{bb}_4 \equiv \bar{\Psi}_b \gamma_4 \Psi_b. \tag{6}$$

2pt function analysis

- Generate zero momentum meson propagators and do the multi-states fitting [Sungwoo Park, et al., Lattice 2018]

$$C^{2\text{pt}}_{B(\text{or } D^*)}(t,\mathbf{0}) = |\mathcal{A}_0|^2 e^{-M_0 t}\left(1 + \left|\frac{\mathcal{A}_2}{\mathcal{A}_0}\right|^2 e^{-\Delta M_2 t} + \left|\frac{\mathcal{A}_4}{\mathcal{A}_0}\right|^2 e^{-(\Delta M_2+\Delta M_4)t} + \cdots \right.$$
$$\left. - (-1)^t\left|\frac{\mathcal{A}_1}{\mathcal{A}_0}\right|^2 e^{-\Delta M_1 t} - (-1)^t\left|\frac{\mathcal{A}_3}{\mathcal{A}_0}\right|^2 e^{-(\Delta M_1+\Delta M_3)t} + \cdots \right) + (t \leftrightarrow T - t)$$

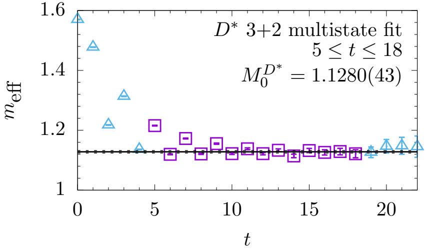

(a) $m_{\text{eff}}(t) \equiv \frac{1}{2}\ln|C^{2pt}(t)/C^{2pt}(t+2)|$.

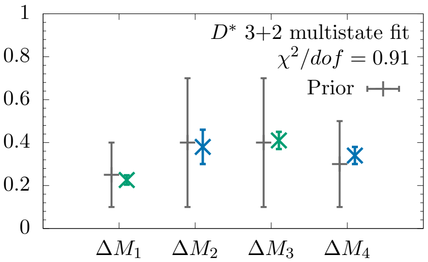

(b) The excited state masses.

3pt function analysis

- Fit 3-point function including 2+1 states for $|B_m\rangle$ and $|D_n^*\rangle$ with $n, m = 0, 1, 2$.

$$
\begin{aligned}
C_{A_j}^{B\to D^*}(t_s,\tau) = {} & \mathcal{A}_0^{D^*}\mathcal{A}_0^{B}\langle D_0^*|A_j^{cb}|B_0\rangle e^{-M_{B_0}(\tau-t_s)}e^{-M_{D_0^*}t_s} \\
& - \mathcal{A}_0^{D^*}\mathcal{A}_1^{B}\langle D_0^*|A_j^{cb}|B_1\rangle(-1)^{(\tau-t_s)}e^{-M_{B_1}(\tau-t_s)}e^{-M_{D_0^*}t_s} \\
& - \mathcal{A}_1^{D^*}\mathcal{A}_0^{B}\langle D_1^*|A_j^{cb}|B_0\rangle(-1)^{t_s}e^{-M_{B_0}(\tau-t_s)}e^{-M_{D_1^*}t_s} \\
& + \mathcal{A}_1^{D^*}\mathcal{A}_1^{B}\langle D_1^*|A_j^{cb}|B_1\rangle(-1)^{\tau}e^{-M_{B_1}(\tau-t_s)}e^{-M_{D_1^*}t_s} \\
& + \mathcal{A}_2^{D^*}\mathcal{A}_0^{B}\langle D_2^*|A_j^{cb}|B_0\rangle e^{-M_{B_0}(\tau-t_s)}e^{-M_{D_2^*}t_s} \\
& + \mathcal{A}_0^{D^*}\mathcal{A}_2^{B}\langle D_0^*|A_j^{cb}|B_2\rangle e^{-M_{B_2}(\tau-t_s)}e^{-M_{D_0^*}t_s} \\
& - \mathcal{A}_2^{D^*}\mathcal{A}_1^{B}\langle D_2^*|A_j^{cb}|B_1\rangle(-1)^{\tau-t_s}e^{-M_{B_1}(\tau-t_s)}e^{-M_{D_2^*}t_s} \\
& - \mathcal{A}_1^{D^*}\mathcal{A}_2^{B}\langle D_1^*|A_j^{cb}|B_2\rangle(-1)^{t}e^{-M_{B_2}(\tau-t_s)}e^{-M_{D_1^*}t_s} \\
& + \mathcal{A}_0^{D^*}\mathcal{A}_2^{B}\langle D_0^*|A_j^{cb}|B_2\rangle e^{-M_{B_2}(\tau-t_s)}e^{-M_{D_0^*}t_s} + \cdots
\end{aligned}
\tag{7}
$$

- In the fitting, the 2pt amplitudes $\mathcal{A}$ and masses M are constant fixed from the 2-point function analysis.

Fitting results for the 3-point correlation functions (1)

$$\mathcal{G}(t,\tau) \equiv \frac{C_{A_j}^{X\to Y}(t,\tau)}{\mathcal{A}_0^Y \mathcal{A}_0^X e^{-M_{X_0}(\tau-t)} e^{-M_{Y_0}t}} = \langle Y_0 | A_j^{cb} | X_0 \rangle + \cdots ,$$

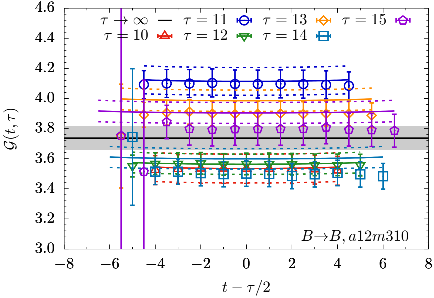

(c) $B \to B$

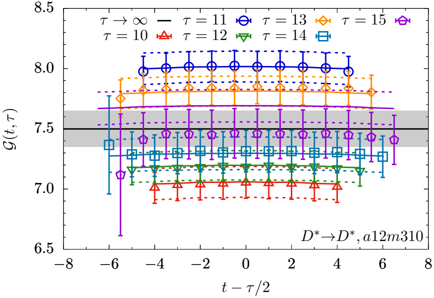

(d) $D^* \to D^*$

[Sungwoo Park, et al., Lattice 2018]

Fitting results for the 3-point correlation functions (2)

$$\mathcal{G}(t,\tau) \equiv \frac{C^{X\to Y}_{A_j}(t,\tau)}{\mathcal{A}^Y_0 \mathcal{A}^X_0 e^{-M_{X_0}(\tau-t)} e^{-M_{Y_0} t}} = \langle Y_0 | A^{cb}_j | X_0 \rangle + \cdots ,$$

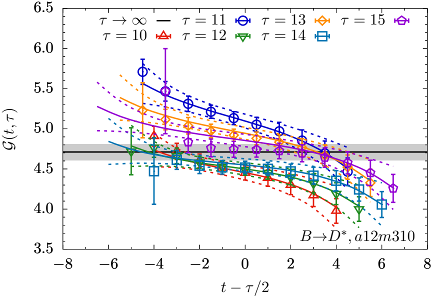

(e) $B \to D^*$

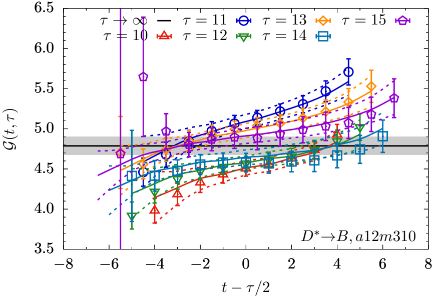

(f) $D^* \to B$

[Sungwoo Park, et al., Lattice 2018]

$\bar{B} \to D^* \ell \bar{\nu}$ Form Factor at Zero Recoil : $h_{A_1}(w = 1)$

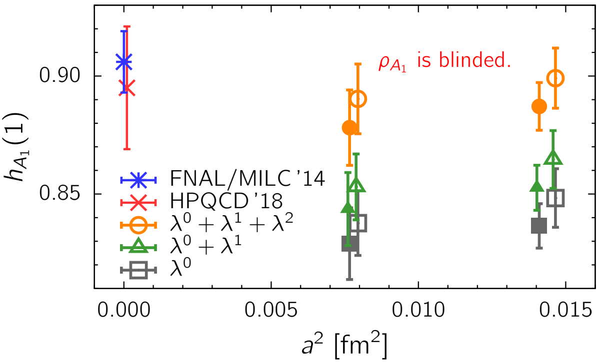

- ρ_{A_j} is blinded: $\rho_{A_j}^2 = \dfrac{Z_{A_j}^{bc} Z_{A_j}^{cb}}{Z_{V_4}^{bb} Z_{V_4}^{cc}} \to 1.$
- Non-perturbative calculation of ρ_{A_j} is underway.
- Preliminary results!!!

$\bar{B} \to D\ell\bar{\nu}$ Form Factors: $h_\pm(w)$ on the lattice

$$\frac{\langle D(M_D, \boldsymbol{p}')|V_\mu|B(M_B, \mathbf{0})\rangle}{\sqrt{2M_D}\sqrt{2M_B}} = \frac{1}{2}\left\{h_+(w)(v+v')_\mu + h_-(w)(v-v')_\mu\right\} ,$$

- B meson is at rest: $v = \dfrac{p}{M_B} = (1, \mathbf{0})$.
- D meson is moving with velocity: $v' = \dfrac{p'}{M_D} = (\dfrac{E_D}{M_D}, \dfrac{\boldsymbol{p}'}{M_D})$.
- Recoil parameter: $w = v \cdot v' = \frac{E_D}{M_D}$.

$\bar{B} \to D\ell\bar{\nu}$ Form Factors $h_\pm(w)$

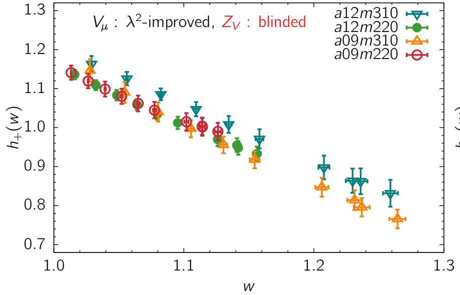

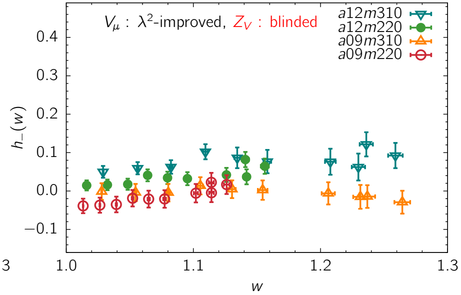

- MILC HISQ lattices at $a \cong 0.12$fm and $a \cong 0.09$fm
- Z_V is blinded. (NPR is underway.)
- The vector current is improved up to the λ^2 order.
- Preliminary results!!!

Summary

- This is the first numerical study with the OK action using the currents improved up to $\mathcal{O}(\lambda^3)$.
- We produced 3-point correlation functions, and obtained preliminary results for $\frac{|h_{A_1}(1)|}{\rho_{A_j}}$ $(\bar{B} \to D^* \ell \bar{\nu})$ and $\frac{h_\pm(w)}{Z_V}$ $(\bar{B} \to D \ell \bar{\nu})$.

[To do list]

- Non-perturbative (NPR) calculation of matching factors: ρ_{A_j}, Z_V.
- Extend measurement to superfine ($a \sim 0.06$fm), and ultrafine ($a \sim 0.045$fm) ensembles and accumulate more statistics.
- Chiral-continuum extrapolation (get results at $a \to 0$)
- Calculate $R(D)$ and $R(D^*)$
- Calculate beyond the standard model contributions from scalar or tensor type currents.